

Modelling of a tuned liquid multi-column damper. Application to floating wind turbine for improved robustness against wave incidence

Christophe Coudurier, Olivier Lepreux, Nicolas Petit

► To cite this version:

Christophe Coudurier, Olivier Lepreux, Nicolas Petit. Modelling of a tuned liquid multi-column damper. Application to floating wind turbine for improved robustness against wave incidence. Ocean Engineering, Elsevier, 2018, 165, pp.277 - 292. 10.1016/j.oceaneng.2018.03.033 . hal-01865061

HAL Id: hal-01865061

<https://hal-mines-paristech.archives-ouvertes.fr/hal-01865061>

Submitted on 24 Oct 2018

HAL is a multi-disciplinary open access archive for the deposit and dissemination of scientific research documents, whether they are published or not. The documents may come from teaching and research institutions in France or abroad, or from public or private research centers.

L'archive ouverte pluridisciplinaire **HAL**, est destinée au dépôt et à la diffusion de documents scientifiques de niveau recherche, publiés ou non, émanant des établissements d'enseignement et de recherche français ou étrangers, des laboratoires publics ou privés.

1
2
3
4 Modelling of a Tuned Liquid Multi-Column Damper.
5 Application to floating wind turbine for improved
6 robustness against wave incidence
7
8
9

10 Christophe Coudurier^b, Olivier Lepreux^a, Nicolas Petit^b

11
12 ^a*IFP Energies nouvelles, Rond-point de l'échangeur de Solaize, BP 3, 69360 Solaize,*
13 *France, e-mail: olivier.lepreux@ifpen.fr*

14 ^b*MINES ParisTech, Centre Automatique et Systèmes, Unité Mathématiques et Systèmes,*
15 *60 Bd St-Michel, 75272 Paris, Cedex 06, France, e-mails:*
16 *christophe.coudurier@mines-paristech.fr, nicolas.petit@mines-paristech.fr*
17
18
19

20 **Abstract**

21
22 In this paper, the coupling of a float with a tuned liquid multi-column damper
23 (TLMCD), a novel structural damping device inspired by the classical tuned
24 liquid column damper (TLCD), is modelled using Lagrangian mechanics. We
25 detail the tuning of the design parameters for each considered variant of the
26 TLMCD, and compare each of them against a layout of multiple TLCDs. The
27 results show that the proposed TLMCD is superior to multiple TLCDs for this
28 application as it is more robust against wave incidence and it creates significantly
29 less parasitic oscillations.
30
31

32 **1. Introduction**

33
34 Wind power is the second fastest growing source of renewable electricity
35 [19] in terms of installed power. The construction of offshore wind farms is
36 growing worldwide. In Europe, offshore wind energy is expected to grow to 23.5
37 GW by 2020, tripling the installed capacity in 2015 [5]. The major causes of
38 this recent trend are the strength and regularity of wind far from the shore,
39 which should allow for the easy mass production of electricity. To generate
40 offshore wind energy, two types of technologies have been considered: fixed-
41 bottom wind turbines (foundations fixed into the seabed) and floating wind
42 turbines (FWTs). The fixed-bottom offshore wind turbine technology is too
43 costly for use in water deeper than 60 m [16]. This disqualifies them from use
44 in most seas. FWTs are a tempting alternative. One advantage is that FWTs
45 are not as dependent on seabed conditions for installation and can be moved to
46 a harbour for maintenance. The main drawback of FWTs is their sensitivity to
47 surrounding water waves that increase the mechanical load on the wind turbine
48 [10], hence reducing the lifespan of its mechanical parts. This sensitivity can be
49 mitigated by increasing the mass and size of the mechanical structure. However,
50 this leads to a prohibitive rise in the cost per kWh.
51

52
53 Previous studies have proposed compensating for tower fore-aft oscillations
54 using collective and individual blade pitch control to modify the wind thrust
55 forces [10, 17, 2]. This solution has the advantage of requiring no structural
56 modification, but delivers limited performance. The tower movements are still
57
58

1
2
3
4
5 many times superior to those observed on onshore wind turbines. Instead of
6 using aerodynamic forces, it is tempting to consider using hydrodynamic forces.
7 In naval engineering, considerable attention has been paid to ship roll damping
8 (since the advent of steamboats). However, most solutions involve the use of
9 the speed of the ship relative to the water to generate lift to control the roll [20]
10 and, for this reason, are not easily transferable to our problem.

11 In addition to naval engineering, civil engineering has been a great contrib-
12 utor to such approaches, as skyscrapers are highly sensitive to wind gusts and
13 earthquakes. This general field (*structural control*) is beyond the scope of this
14 paper, and the reader can refer to [21] for an overview. To improve the response
15 of massive structures to external disturbances, attached moving masses, such
16 as tuned mass dampers (TMD), can be employed. Among the most economical
17 and efficient solutions is the tuned liquid column damper (TLCD), also known
18 as the anti-roll tank or the U-tank. As originally proposed by Frahm [6, 15] to
19 limit ship roll, it is a U-shaped tube on a plane orthogonal to the ship's roll
20 axis, and is generally filled with water. The liquid inside the TLCD oscillates
21 due to the movement of the structure and liquid's energy is dissipated through
22 a restriction located in the horizontal section. The TLCD is usually chosen to
23 damp the natural frequency of the structure. While TLCD systems have been
24 modelled in the past by, for instance, [1, 7], it remains an active field of research
25 [4]. A considerable amount of relevant research has been conducted over the
26 last two decades on civil engineering applications, where most of the work has
27 focused on determining the optimal design of passive TLCDs, such as [7, 25, 26].

28 Several studies have shown that the structural control of floating wind tur-
29 bines using active [11, 18] or passive [24, 23] TMDs can substantially reduce the
30 load on the wind turbine. Other studies [3, 14, 22] have shown that the passive
31 and semi-active TLCDs are an interesting alternative.

32 In this paper, we consider the damping of an offshore platform subject to
33 waves of various angles of incidence. Such a system behaves as a six-DOF peri-
34 odically oscillating rigid body. We try to minimize the roll and pitch oscillations
35 by means of a TLCD, and neglect aerodynamic forces. Due to the mooring sys-
36 tem, we cannot easily change the orientation of the float to adapt to the wave
37 incidence. In the past, we studied the disturbance rejection capabilities of a
38 TLCD aligned with the wave incidence [3]. As shown in Fig. 1, the damping
39 provided by the TLCD is not robust against a change in the wave incidence.

40 This work is partly based on [8]. However, unlike the ships considered there,
41 the float we consider has isotropic properties, meaning that its roll and pitch
42 motions have the same characteristics. Here we go a step further introducing
43 three multidirectional damping devices based on the concept of the TLCD. Their
44 dynamics and their robustness against wave incidence are investigated.

45 2. Description of the system

46 The floater considered was the MIT/NREL Shallow Drafted Barge and the
47 wind turbine was an NREL 5 MW; both are described in Tables 2 and 3.
48 The barge and the wind turbine are modelled as a single rigid body, referred
49 to as “the float” in this paper. Deformations in the wind turbine are neglected
50 as its resonant period is inferior to the period of the monochromatic waves we
51 consider here – ranging from 3 s to 30 s. The float is studied with all six degrees
52 of freedom. To avoid any bias in the study, we do not consider the interaction
53
54
55
56
57
58

\mathcal{R}_n	Earth-fixed frame
\mathcal{R}_b	Barge-fixed frame
$R(\Theta) \in \mathbb{R}^{3 \times 3}$	Rotation matrix from \mathcal{R}_b to \mathcal{R}_n so that $\forall r \in \mathbb{R}^3, r^n = Rr^b$
$x^n = [x, y, z]^\top \in \mathbb{R}^3$	Position of the centre of gravity of barge in \mathcal{R}_n
$\Theta = [\varphi, \theta, \psi]^\top \in \mathbb{R}^3$	Euler triple associated with R
$v^b \in \mathbb{R}^3$	Speed of CoG , the centre of gravity of the float
$\omega^b \in \mathbb{R}^3$	Rotational speed of \mathcal{R}_b with respect to \mathcal{R}_n
nc	Number of variables needed to describe the liquid speed in the TLCD/TLMCD
$w \in \mathbb{R}^{nc}$	Vector describing the position of the liquid in the TLMCD
$w_i \in \mathbb{R}$	position of the liquid in the i^{th} element
$q = [x^n^\top, \Theta^\top, w^\top]^\top \in \mathbb{R}^{6+nc}$	System's generalized positions
$v = [v^b^\top, \omega^b^\top, \dot{w}^\top]^\top \in \mathbb{R}^{6+nc}$	System's speeds
$G(\Theta) \in \mathbb{R}^{3 \times 3}$	Matrix relating $\dot{\Theta}$ and ω^b so that $\omega^b = G\dot{\Theta}$
$\mathcal{P}(\Theta) \in \mathbb{R}^{6+nc \times 6+nc}$	Matrix relating \dot{q} and v so that $v = \mathcal{P}\dot{q}$
$S(\cdot) \in \mathbb{R}^{3 \times 3}$ $S^2(\cdot) = S(\cdot)^\top S(\cdot)$	Skew symmetric matrix representing the cross-product in \mathbb{R}^3 , with $S(x)y = x \times y$.
A_v and $A_h \in \mathbb{R}$	Cross-sections of the vertical and horizontal tubes of the tank
$\nu \in \mathbb{R}$	Cross-section ratio defined as $\nu \triangleq A_v/A_h$
$\sigma_i \in \mathbb{R}$	Curvilinear abscissa describing the geometry of the i^{th} element
$\varsigma_i, \varsigma_{pi}, \varsigma_{si} \in \mathbb{R}$	Abscissa of the free surfaces in the i^{th} element
$\alpha_i \in \mathbb{R}$	orientation angle of the i^{th} element
$r^b(\sigma) = [x_t^b, y_t^b(\sigma), z_t^b(\sigma)]^\top \in \mathbb{R}^3$	Function describing the centreline of the damper
$A(\sigma) > 0 \in \mathbb{R}$	Cross-section of the tank at abscissa σ
L_v and $L_h \in \mathbb{R}$	Length of the vertical and horizontal tubes of the TLCD
$e \in \mathbb{R}$	Distance between CoG and the horizontal tubes
$\rho \in \mathbb{R}$	Liquid density
$\eta \in \mathbb{R}^{nc}$	Vector of the head-loss coefficients of the restrictions
$M_s = M_s^\top \in \mathbb{R}^{6 \times 6}$	Mass matrix of the float
$m_t \in \mathbb{R}$	Total mass of the liquid in the damping system
$Q_{hydro} \in \mathbb{R}^6$	Generalized force due to the barge/waves interactions
$Q_{res} \in \mathbb{R}^{nc}$	Generalized force due to the restrictions in the TLMCD
$F_h \in \mathbb{R}^N$	Force generated by the fluid flow through the restrictions
$\beta \in \mathbb{R}$	Wave incidence angle

Table 1: Nomenclature

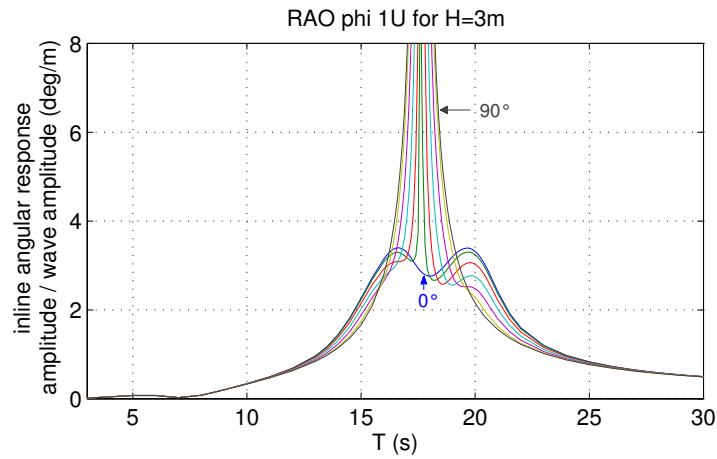


Figure 1: RAO of the float damped by a single TLCD for different incident angles

Diameter, Height	36 m, 9.5 m
Draft, Freeboard	5 m, 4.5 m
Water Displacement	5,089 m ³
Mass, Including Ballast	4,519,150 kg
CM Location below SWL	3.88238 m
Roll Inertia about CM	390,147,000 kg.m ²
Pitch Inertia about CM	390,147,000 kg.m ²
Yaw Inertia about CM	750,866,000 kg.m ²
Anchor (Water) Depth	200 m
Separation between Opposing Anchors	436 m
Unstretched Line Length	279.3 m
Neutral Line Length Resting on Seabed	0 m
Line Diameter	0.127 m
Line Mass Density	116 kg/m
Line Extensional Stiffness	1,500,000,000 N

Table 2: Summary of MIT / NREL Barge Properties, from [10]

Rating	5 MW
Rotor Orientation, Configuration	Upwind, 3 Blades
Control Variable Speed	Collective Pitch
Drivetrain High Speed	Multiple-Stage Gearbox
Rotor, Hub Diameter	126 m, 3 m
Hub Height	90 m
Cut-In, Rated, Cut-Out Wind Speed	3 m/s, 11.4 m/s, 25 m/s
Cut-In, Rated Rotor Speed	6.9 rpm, 12.1 rpm
Rated Tip Speed	80 m/s
Overhang, Shaft Tilt, Precone	5 m, 5°, 2.5°
Rotor Mass	110,000 kg
Nacelle Mass	240,000 kg
Tower Mass	347,460 kg
Coordinate Location of Overall CM	(-0.2 m, 0.0 m, 64.0 m)

Table 3: Gross Properties Chosen for the NREL 5-MW Baseline Wind Turbine, from [10]

between the rotor and the wind because the damping induced is dependent on the controller chosen for the wind turbine (its impact can be negative or positive [13]). An illustration of the float with a 3S TLMCD is given in Figure 2.

2.1. Assumptions

To model the dynamics of the tank, we make the following assumptions:

1. the float is rigid. Therefore,
2. its centre of gravity, CoG, is immobile in the frame fixed to the barge,
3. the liquid in the TLCD is incompressible,
4. the column width is small with respect to length,
5. the flow of liquid in the tank is uniform in each column,
6. the position of the free surface of liquid in the tank is within the vertical column (i.e. vertical columns are never empty).

2.2. Kinematics of the tank

A TLCD is composed of two vertical tanks of cross-section A_v connected by a horizontal duct of cross-section A_h . Liquid flows from one vertical column to the other through the horizontal tube. The restriction causing the damping (head loss) is located in the middle of the horizontal part. Fig. 3 is an illustration of the TLCD with the parameters presented in this subsection.

As we neglect the width of the columns, the TLCD geometry is defined by a line whose coordinates are expressed in the frame fixed to the barge

$$r^b(\sigma) \triangleq [x_t^b, y_t^b(\sigma), z_t^b(\sigma)]^T$$

with

$$y_t^b(\sigma) \triangleq \begin{cases} \frac{L_h}{2} & \sigma \leq -\frac{L_h}{2} \\ -\sigma & -\frac{L_h}{2} < \sigma \leq \frac{L_h}{2} \\ -\frac{L_h}{2} & \frac{L_h}{2} < \sigma \end{cases} \quad z_t^b(\sigma) \triangleq \begin{cases} e + \frac{L_h}{2} + \sigma & \sigma \leq -\frac{L_h}{2} \\ e & -\frac{L_h}{2} < \sigma \leq \frac{L_h}{2} \\ e + \frac{L_h}{2} - \sigma & \frac{L_h}{2} < \sigma \end{cases}$$



Figure 2: Illustration of the float with a 3S TLMCD

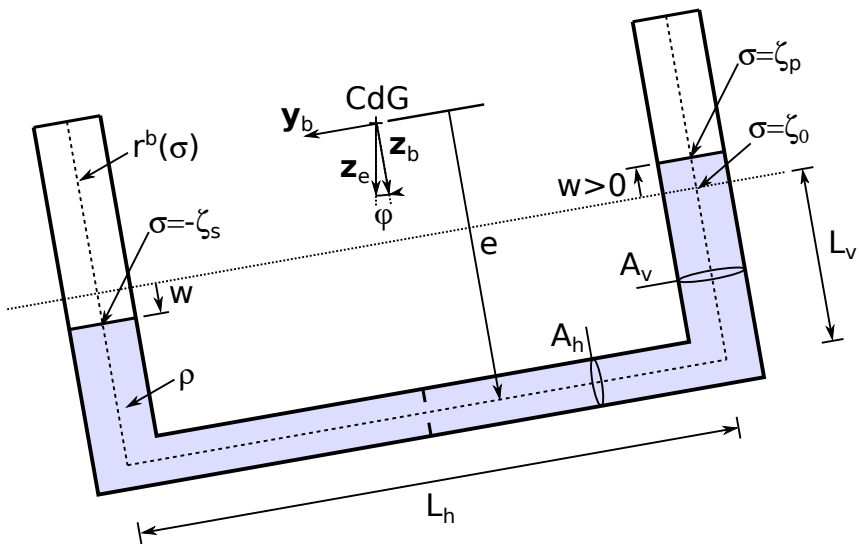


Figure 3: Scheme of a single TLMCD illustrating the main variables

1
2
3
4
5 where x_t^b is defined for each damping system to generate a symmetric problem,
6 and where σ is the curvilinear abscissa along the geometry of the tank ($\sigma = 0$ is
7 at the centre of the horizontal tube, and for $\sigma > 0$ $y_t^b(\sigma)$ is negative). We write
8 $\frac{d\mathbf{r}^b}{d\sigma}(\sigma)$ as the unit vector tangent to the tank.
9

We define the cross-sectional area of the tank as

$$10 \quad A(\sigma) \triangleq \begin{cases} A_v & \sigma \leq -\frac{L_h}{2} \\ A_h & -\frac{L_h}{2} < \sigma \leq \frac{L_h}{2} \\ A_v & \frac{L_h}{2} < \sigma \end{cases}$$

11
12
13
14
15 In this paper, the damping systems we consider consist of N identical ele-
16 mentary subsystems (referred to as elements), which are regularly rotated around
17 (CoG, \mathbf{z}_b) . The geometry of each element is given by $R_z(\alpha_i) r^b(\sigma_i)$ where
18

$$19 \quad R_z(\alpha_i) = \begin{bmatrix} \cos(\alpha_i) & -\sin(\alpha_i) & 0 \\ \sin(\alpha_i) & \cos(\alpha_i) & 0 \\ 0 & 0 & 1 \end{bmatrix}$$

20
21
22
23 is the rotation matrix around \mathbf{z} and where α_i is the orientation angle of the i^{th}
24 element. Let $v_i(\sigma_i)$ be the algebraic speed in in the i^{th} element of the damping
25 system. By convention, $v_i(\sigma_i)$ is positive if the liquid flows towards positive σ .
26 The vector $\mathbf{v}_i^b(\sigma_i)$ is the speed of the liquid in the i^{th} element expressed in \mathcal{R}_b
27 as
28

$$29 \quad \mathbf{v}_i^b(\sigma_i) = v_i(\sigma_i) R_z(\alpha_i) \frac{d\mathbf{r}^b}{d\sigma}(\sigma_i) \quad (1)$$

30
31 We also introduce \mathcal{V}_h , the vector of algebraic speeds in the horizontal tubes,
32 as

$$33 \quad \mathcal{V}_h \triangleq \begin{bmatrix} v_1(0) \\ \vdots \\ v_N(0) \end{bmatrix}$$

$$34 \quad \mathcal{V}_h = P_h \dot{w} \quad (2)$$

35
36
37 with P_h given for each damping system in the Appendices.
38
39

40 3. Linearised dynamics

41
42 We define $X \triangleq [\mathbf{x}^n \quad \Theta \quad w \quad \dot{\mathbf{x}}^n \quad \dot{\Theta} \quad \dot{w}]^\top$ the state vector of our system,
43 with $x^n = [x, y, z]^\top \in \mathbb{R}^3$ the position of the systems centre of gravity, $\Theta =$
44 $[\varphi, \theta, \psi]^\top \in \mathbb{R}^3$ the orientation of the float, $w \in \mathbb{R}^{nc}$ and nc the number of
45 variables describing the speed of the liquid inside the TLCD (nc will be detailed
46 in §4 for each variant). The linearised model writes
47
48

$$49 \quad \dot{X} = \mathcal{A}(\omega) X + \mathcal{B}(\omega) \begin{bmatrix} F_{hydro}(\omega, H) \\ Q_{res}(\eta) \end{bmatrix}$$

50
51 with

$$52 \quad \mathcal{A}(\omega) = \begin{bmatrix} 0_{6+nc \times 6+nc} & I_{6+nc \times 6+nc} \\ (M(0) + A(\omega))^{-1} K & (M(0) + A(\omega))^{-1} (C(0, 0) + B(\omega)) \end{bmatrix}$$

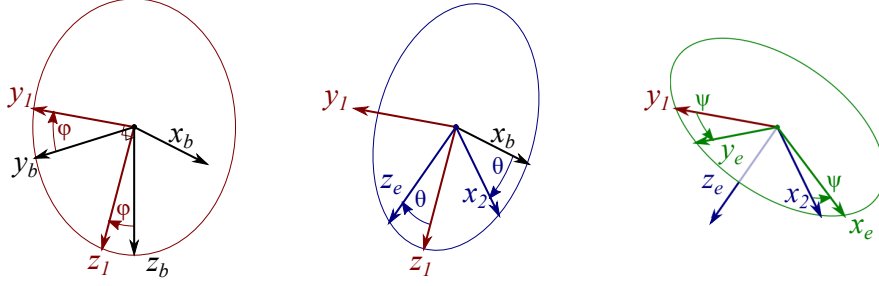


Figure 4: Orientation of \mathcal{R}_b with respect to \mathcal{R}_e

$$\mathcal{B}(\omega) = \begin{bmatrix} 0_{6+nc \times 6+nc} \\ (M(0) + A(\omega))^{-1} \end{bmatrix}$$

where $M(0)$ and $C(0,0)$ the mass matrices given in §4 where $(q, \dot{q}) = 0$. The matrices $A(\omega)$ and $B(\omega)$ are respectively the radiation added mass and damping matrices, with ω the angular frequency of the monochromatic wave. The stiffness matrix K accounts for buoyancy and gravity. The forces applied on the float and the liquid inside the TLCB are $F_{hydro}(\omega, H)$, depending on the angular frequency ω and H the wave height, and $Q_{res}(\eta)$ as given in §4.2.

This linear model is based on the non-linear model presented in §4, which can be skipped by the reader, the system is tuned in §5, and the results of the numerical simulations are given in §6.

4. Dynamic model of the damping systems

4.1. Description and properties of the frames

In this paper, two frames are used: $\mathcal{R}_b \triangleq (CoG, \mathbf{x}_b, \mathbf{y}_b, \mathbf{z}_b)$ is the frame fixed to the barge, and $\mathcal{R}_n \triangleq (O, \mathbf{x}_n, \mathbf{y}_n, \mathbf{z}_n)$ is the Earth-fixed frame. Every vector $r \in \mathbb{R}^3$ is denoted by r^b when expressed in the b frame and r^n in \mathcal{R}_n . The frames are oriented such as \mathbf{z} points downwards.

The orientation of \mathcal{R}_b with respect to \mathcal{R}_n is defined by the “roll-pitch-yaw” Euler triple denoted by $\Theta = [\varphi, \theta, \psi]^\top \in \mathbb{R}^3$. The rotation matrix associated with Θ is

$$R(\Theta) \triangleq \begin{bmatrix} c_\psi c_\theta & -s_\psi c_\theta + c_\psi s_\theta s_\varphi & s_\psi s_\theta + c_\psi s_\theta c_\varphi \\ s_\psi c_\theta & c_\psi c_\theta + s_\psi s_\theta s_\varphi & -c_\psi s_\theta + s_\psi s_\theta c_\varphi \\ -s_\theta & c_\theta s_\varphi & c_\theta c_\varphi \end{bmatrix}$$

with $c_x = \cos(x)$ and $s_x = \sin(x)$. Therefore, $\dot{\mathbf{x}}^n = R\mathbf{v}^b$, where \mathbf{x}^n is the position of CoG in \mathcal{R}_n expressed in the n frame, and \mathbf{v}^b the velocity of \mathcal{R}_b relatively to \mathcal{R}_n and expressed in \mathcal{R}_b . For all $\mathbf{u} = [u_1, u_2, u_3]^\top \in \mathbb{R}^3$, we define the cross-product matrix as

$$S(\mathbf{u}) \triangleq \begin{bmatrix} 0 & -u_3 & u_2 \\ u_3 & 0 & -u_1 \\ -u_2 & u_1 & 0 \end{bmatrix} = -S(\mathbf{u})^\top$$

such that $\forall x, y \in \mathbb{R}^3$, $S(x)y = x \times y$. We denote by ω^b the rotation speed of the b frame relative to the n frame, expressed in \mathcal{R}_b . The time derivative of R can then be given by [12]

$$\dot{R} = RS(\omega^b)$$

We define

$$\begin{aligned} G(\Theta) &\triangleq \begin{bmatrix} \mathbf{x}, R([\varphi, 0, 0]^\top)^\top \mathbf{y}, R(\Theta)^\top \mathbf{z} \end{bmatrix} \\ &= \begin{bmatrix} 1 & 0 & -s_\theta \\ 0 & c_\varphi & s_\varphi c_\theta \\ 0 & -s_\varphi & c_\varphi c_\theta \end{bmatrix} \end{aligned} \quad (3)$$

such that $\omega^b = G\dot{\Theta}$, with \mathbf{x} , \mathbf{y} , \mathbf{z} as the unit vector along each axis.

We define $q \triangleq \begin{bmatrix} \mathbf{x}^n \\ \Theta \\ w \end{bmatrix}$ and $v \triangleq \begin{bmatrix} \mathbf{v}^b \\ \omega^b \\ \dot{w} \end{bmatrix}$, with $w \in \mathbb{R}^{nc}$ and nc the number of variables describing the speed of the liquid inside the TLCD (nc will be detailed in §4 for each variant). These variables are linked via $v = \mathcal{P}\dot{q}$ with

$$\mathcal{P}(\Theta) = \begin{bmatrix} R(\Theta)^\top & 0_{3 \times 3} & 0_{3 \times nc} \\ 0_{3 \times 3} & G(\Theta) & 0_{3 \times nc} \\ 0_{nc \times 3} & 0_{nc \times 3} & \mathbb{I}_{nc} \end{bmatrix}$$

We have described the geometry and kinematics of the system, and now establish the dynamics of our systems using the Lagrangian approach. The dynamics of the system are classically given as

$$\frac{d}{dt} \frac{\partial(T - V)}{\partial \dot{q}} - \frac{\partial(T - V)}{\partial q} = Q$$

with T the kinetic energy, V the potential energy and Q the generalized forces.

4.2. Generalized forces

To obtain Q (the generalized forces), we express the power generated by external forces on our system as $\dot{q}^\top Q$. We write $Q \triangleq Q_{hydro} + Q_{res}$, with Q_{hydro} the generalized force due to the interactions between the waves and the barge, and Q_{res} the generalized force due to the restrictions in the TLMCD. For our simulations, the interactions between the platform and the water were modelled using a diffraction-radiation software. Following classical writing of the force generated by the fluid flow through the restriction, we write the forces $F_h \in \mathbb{R}^N$ in a damping system as

$$F_h = -\frac{1}{2} \rho A_h \eta \circ \mathcal{V}_h(\dot{w}) \circ |\mathcal{V}_h(\dot{w})|$$

with $\eta \in \mathbb{R}^N$ the vector of head-loss coefficients, ρ the fluid density, and \circ the Hadamard product (entrywise product). To establish the expression for Q_{res} , we express the power dissipated by the restrictions as $P_{res} = \mathcal{V}_h^\top F_h$, with $\mathcal{V}_h^\top = \dot{w}^\top P_h^\top$ according to (2). Therefore, Q_{res} is given by

$$Q_{res}(t, \dot{w}) = \begin{bmatrix} 0_{6 \times 1} \\ P_h^\top F_h(\dot{w}) \end{bmatrix} \quad (4)$$

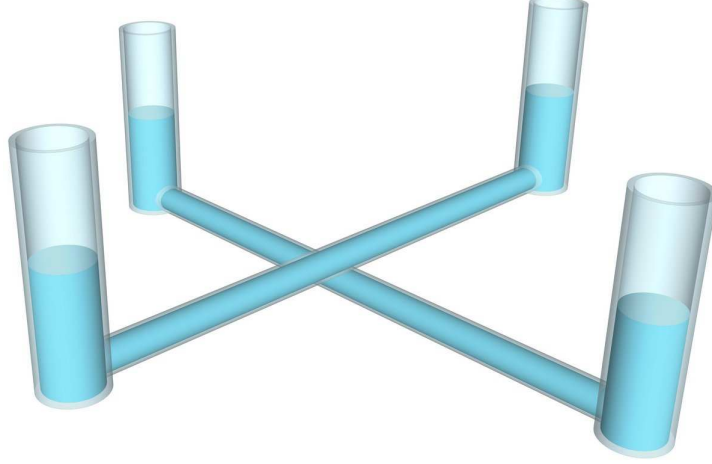


Figure 5: Geometry of the 2U damping system (the tubes do not intersect)

4.3. System with N TLCDs (NU)

We consider N TLCDs regularly rotated around (CoG, \mathbf{z}_b) , and denote this system NU . As an example, the 2U system is illustrated in Fig. 5. We set $x_t^b = 0$ for our system to be axisymmetric. The orientation angle of each element writes $\alpha_i = \pi \frac{i-1}{N}$. To describe the position of the liquid, we need N variables, i.e. $nc = N$. For the NU system, each element is a TLCD, therefore, the curvilinear abscissa of each element, σ_i , ranges from $-\varsigma_{si}$ to ς_{pi} defined as

$$\begin{aligned}\varsigma_{pi} &= \frac{L_h}{2} + L_v + w_i \\ \varsigma_{si} &= \frac{L_h}{2} + L_v - w_i\end{aligned}$$

4.3.1. Mechanical energy of the system

The potential energy of the NU system is written as

$$\begin{aligned}V_{NU} &= \mathbf{z}^\top \cdot \left(g\rho \sum_{i=1}^N \int_{-\varsigma_{si}}^{\varsigma_{pi}} A_t(\sigma) (R(\Theta) R_z(\alpha_i) \mathbf{r}^b(\sigma) + \mathbf{x}^n) d\sigma \right) \\ &= -gm_t z - g\rho \mathbf{z}^\top R(\Theta) \left[\rho \sum_{i=1}^N \int_{-\varsigma_{si}}^{\varsigma_{pi}} A_t(\sigma) R_z(\alpha_i) \mathbf{r}^b(\sigma) d\sigma \right]\end{aligned}\quad (5)$$

where g is the acceleration due to gravity, m_t is the total mass of the liquid in the damping system.

The kinetic energy of the system is written as

$$T_{NU} = \frac{1}{2} \dot{q}^\top \mathcal{M}_{NU}(q) \dot{q}\quad (6)$$

with

$$\mathcal{M}_{NU}(q) \triangleq \mathcal{P}(\Theta)^\top M_{NU}(w) \mathcal{P}(\Theta) = \mathcal{M}_{NU}^\top \in \mathbb{R}^{6+nc \times 6+nc}\quad (7)$$

with $M_{NU}(w)$ as defined in (A.2). The calculation of the kinetic energy is detailed in Appendix A.1.

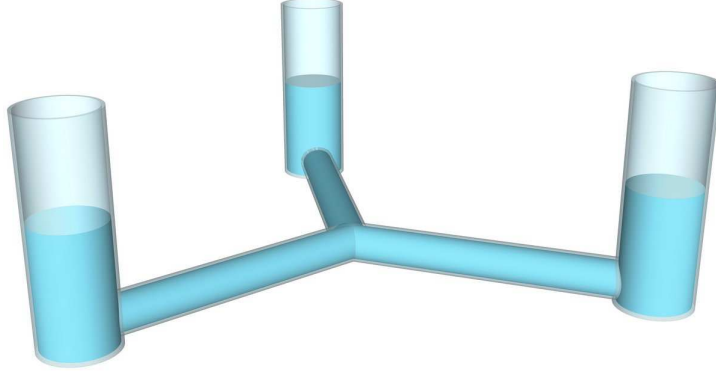


Figure 6: The 3S TLMCD

4.3.2. System dynamics

We write the dynamics of the system as

$$\mathcal{M}_{NU}(q) \ddot{q} + C_{NU}(q, \dot{q}) \dot{q} + k_{NU}(q) = Q_{hydro} + Q_{res_{NU}}(\dot{w}) \quad (8)$$

with $\mathcal{M}_{NU}(q)$ as defined in (7), and C_{NU} , k_{NU} and $Q_{res_{NU}}$ as defined in Appendix B.3.

4.4. Model of a star-shaped TLMCD with N elements (NS)

This damping system is composed of N halves of the TLCD interconnected at the coordinate \mathbf{r}^b ($\sigma = 0$) and regularly rotated around (CoG, \mathbf{z}_b). We denote this system NS . For illustration purpose, the 3S system is shown in Fig. 6. For this system, each element is a half-TLCD, therefore the curvilinear abscissa of each element, σ_i , ranges from 0 to ς_i . We still consider $x_t^b = 0$. The orientation angle writes, $\alpha_i = \frac{2\pi(i-1)}{N}$.

We note $\sigma = \varsigma_i$, the coordinate of the free surface of the i^{th} element. The total mass of the liquid is constant, and can be given by

$$m_t \triangleq \rho \sum_{i=1}^N \int_0^{\varsigma_i} A_t(\sigma_i) d\sigma_i$$

If we know ς_i for $i = 1, \dots, N-1$, we can easily deduce ς_N ; therefore, $nc = N-1$. We define, for $i = 1..nc$,

$$\varsigma_i = \frac{L_h}{2} + L_v + w_i, \quad (9)$$

and

$$\varsigma_N = \frac{L_h}{2} + L_v - \sum_{i=1}^{N-1} w_i. \quad (10)$$

As shown in Appendix B.4, we write the dynamics of the system as

$$\mathcal{M}_{NS}(q) \ddot{q} + C_{NS}(q, \dot{q}) \dot{q} + k_{NS}(q) = Q_{hydro} + Q_{res_{NS}}(\dot{w}) \quad (11)$$

where \mathcal{M}_{NS} , C_{NS} , k_{NS} and $Q_{res_{NS}}$ are defined in Appendix B.4.

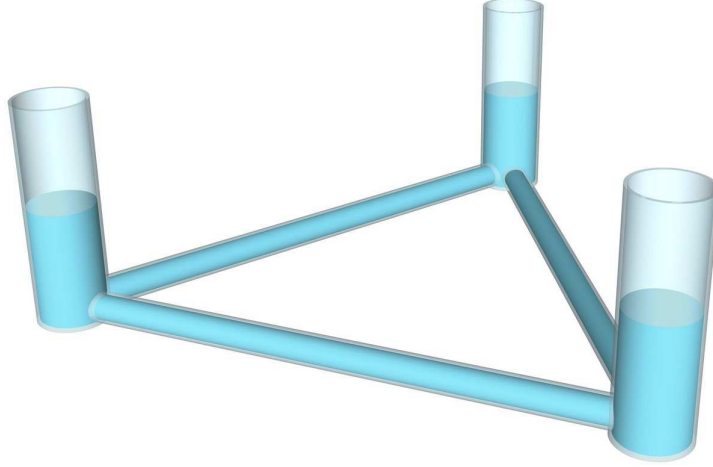


Figure 7: The 3P TLMCD

4.5. Model of polygonal TLMCD with N elements (NP)

This damping system is composed of N horizontal columns laid out to form a convex regular N -gon with N vertical columns positioned at each intersection. We denote this system NP. The 3P case is shown in Fig. 7. The elements of this system are composed of one horizontal tube and one vertical column, therefore, the curvilinear abscissa of each element, σ_i , ranges from $-\frac{L_h}{2}$ to ζ_i , as defined in (9). The geometry of our system implies $x_t^b = -\frac{L_h}{2 \tan \frac{\pi}{N}}$. The orientation angle α_i writes $\alpha_i = \frac{2\pi(i-1)}{N}$, as in the NS problem.

There are $2N$ values of the speed of the liquid (one for each horizontal tube and each vertical column). We can write N local relations of flow conservation (at the base of each vertical column). We need $nc = 2N - N = N$ independent variables to know the speed of the liquid in each column. As the total mass of the liquid is constant, there are $N - 1$ independent positions of free surfaces; therefore, we need to introduce an additional variable to completely describe the system. We arbitrarily choose w_{nc} to be the “position” of the liquid in the N^{th} horizontal column.

The system’s equations of motion are written as

$$\mathcal{M}_{NP}(q) \ddot{q} + C_{NP}(q, \dot{q}) \dot{q} + k_{NP}(q) = Q_{hydro} + Q_{res_{NP}}(\dot{w}) \quad (12)$$

where \mathcal{M}_{NP} , C_{NP} , k_{NP} and $Q_{res_{NP}}$ are defined in Appendix B.5.

4.6. Results frame

As we change the incidence of the waves, we need to change the results variables: we introduce φ_r the inline angular response and θ_r the transverse angular response to describe the oscillations of the FWT along the direction of the waves and perpendicular to the waves, respectively. We need to express φ_r and θ_r in terms of φ , θ and ψ . For this purpose, we introduced \mathcal{R}_{er} and \mathcal{R}_{br} as the “results frames”. They are related via $R(\Theta_r)$ such that $\forall \mathbf{r} \in \mathbb{R}^3$,

$$\mathbf{r}^{er} = R(\Theta_r) \mathbf{r}^{br} \quad (13)$$

where $\Theta_r \triangleq [\varphi_r, \theta_r, \psi_r]^\top$. These frames are linked to \mathcal{R}_e and \mathcal{R}_b by a rotation around \mathbf{z} at angle β , such that $\forall \mathbf{r} \in \mathbb{R}^3$,

$$\mathbf{r}^e = R_z(\beta) \mathbf{r}^{er}$$

and

$$\mathbf{r}^b = R_z(\beta) \mathbf{r}^{br}.$$

In §4.1 we defined $R(\Theta)$ so that

$$\mathbf{r}^e = R(\Theta) \mathbf{r}^b$$

thus, we write

$$\mathbf{r}^{er} = R_z^\top(\beta) \mathbf{r}^e = R_z^\top(\beta) R(\Theta) \mathbf{r}^b = R_z^\top(\beta) R(\Theta) R_z(\beta) \mathbf{r}^{br},$$

and by identification with (13), we get

$$R(\Theta_r) = R_z^\top(\beta) R(\Theta) R_z(\beta). \quad (14)$$

Solving this equation yields Θ_r in terms of Θ and β .

5. Tuning the proposed configurations

Prior to assessing the robustness of each solution against wave incidence, we need to determine their design parameters. First, we must determine the mass of the liquid in the damper. We arbitrarily assume that each TLCD of the 2U variant weighs 2% of the total mass of the float, and that each TLMCD weighs 4% of the total mass, i.e. 2U, 3S and 3P have the same mass. According to [27], the price of the system depends on three factors: the loss of space (occupied by the TLCD), additional construction costs, and the amount of steel needed for the tank. Since the space inside the barge has no commercial value, the cost of the loss of space is zero (if the system to damp was a building, the cost due to loss of space would have been the price of the floors occupied by the device). In our case, if the vertical columns were outside the float, additional construction costs would have incurred to ensure the structural integrity of the TLCD. To reduce this cost to zero, we designed the dampers to fit inside the barge. To determine the best design of each damper, we use the MATLAB `fminsearch` optimisation function, with the following performance index to be minimized:

$$P.I. = \max_{T \in [3;30]} (|\varphi|)$$

where $|\varphi|$ is the steady state roll magnitude obtained via a simulation for each period of monochromatic wave (excitation). It is a *min-max* problem where the decision variables are L_h , L_v , ν and η . This problem is solved under constraints $L_h \leq L_{h_{maxi}}$ and $L_v \leq L_{v_{maxi}}$ to fit the damper inside the barge so that the construction cost remains zero. To avoid a violation of assumption 6, we set $L_v = L_{v_{maxi}}$.

In a previous paper [3], we considered damping with a single TLCD using the same float subject to waves in the vertical plan $x_t = 0$. The results showed that the optimal value of L_h was $L_{h_{maxi}}$. Therefore, we chose to set $L_h = L_{h_{maxi}}$ to reduce the number of variables in the optimization problem. As we have

	ν	η	L_h	A_v	μ	$P.I.$
2U	4.06	5.90	32.31 m	5.68 m ²	4%	3.50
3S	4.12	3.43	31.88 m	7.67 m ²	4%	3.57
3P	7.11	10.72	27.61 m	7.65 m ²	4%	3.54

Table 4: Optimal TLMCD parameters for a wave height $H = 3$ m

$L_h = L_{h_{maxi}}$ and $L_v = L_{v_{maxi}}$, the position of the TLMCD inside the barge is imposed.

We define $\mu \triangleq \frac{m_t}{M_{S_{11}}}$ as the ratio of the mass of the liquid in the TLMCD to the total mass of the float. We summarize the design of each damper in Table 4 for a given wave height $H = 3$ m and an incidence of $\beta=0^\circ$. As the natural period of the float is close to the predominant period of extreme sea states (15 s–20 s), we chose the performance index to damp this resonance. Note that for a given site, we could have used an adapted performance index to obtain the design best suited to the conditions of the local sea.

We also note that ν (the cross-section ratio) of the 3P system is much larger, which means that the 3P system has a lower resonant period for the same ν .

6. Simulation results

In the previous section we detailed the design of each damping system. In this section we perform numerical simulations to compare their robustness against wave incidence. As the dampers are tuned to the roll/pitch natural frequency, they have almost no effect on the other motions of the wind turbine. This is why in this section we only deal with the roll and pitch motions.

6.1. Preliminary considerations

Before we perform numerical simulations, let's consider the following points.

Evaluation criterion: The RAO. We introduce the response amplitude operator (RAO). It is defined as the ratio of the system's motion to the wave amplitude causing it, and is represented over a range of (monochromatic) wave periods [9]. It is employed as a quantitative evaluation tool for the rest of the study.

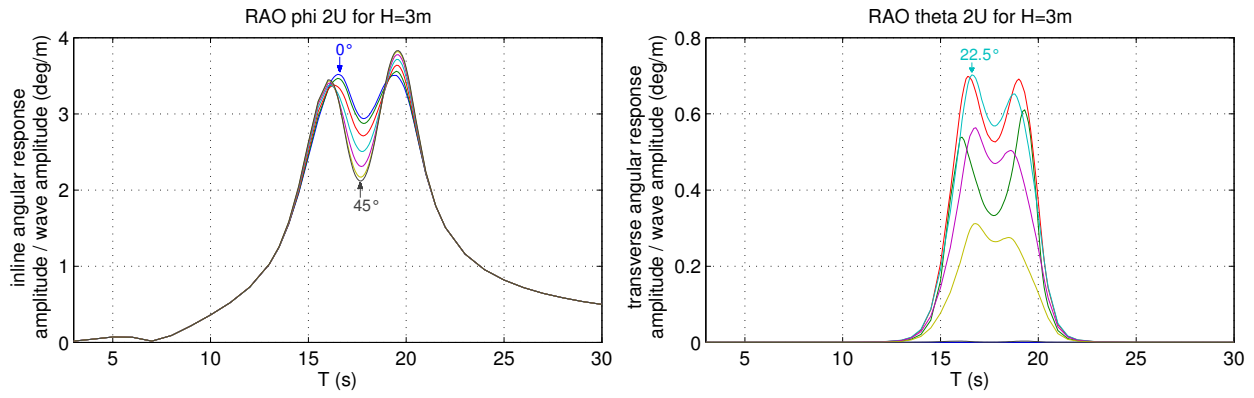
Results frames We remind the reader that we introduced the results frame in §4.6. As we use the linear model, the states of the results frame are linked to the original states via $\mathbf{x}^{nr} = R_z^\top(\beta) \mathbf{x}^n$ and $\Theta^r = R_z^\top(\beta) \Theta$.

6.2. Numerical simulations

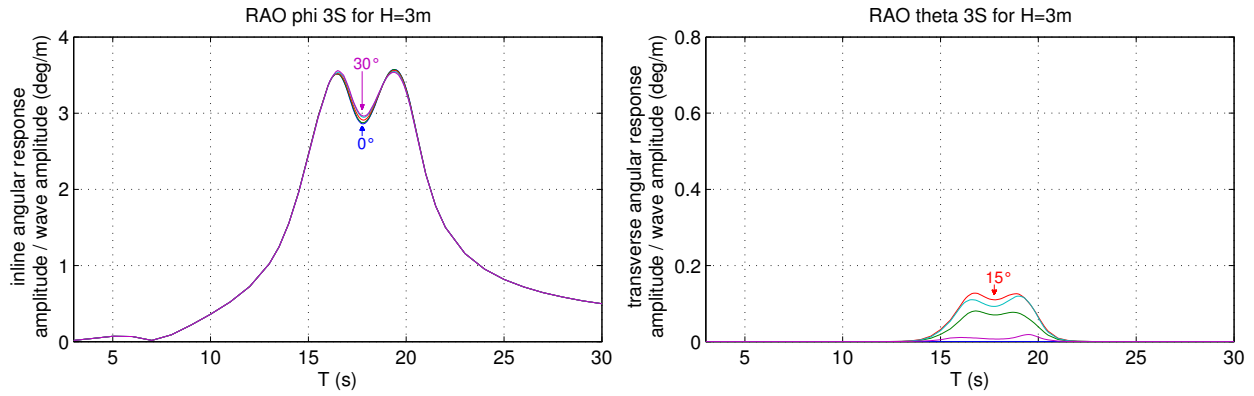
We simulated the system's response to a 3 m wave excitation until a steady state was attained. We plotted the RAOs for monochromatic waves of periods ranging from 3 s to 30 s as well as for different incident angles. It has been verified that the vertical columns were never empty during the simulations.

We plotted the results in Fig. 8. Due to the symmetries of the damping systems, we plotted curves between 0° and 45° for the 2U case, and between 0° and 30° for the 3S and 3P cases.

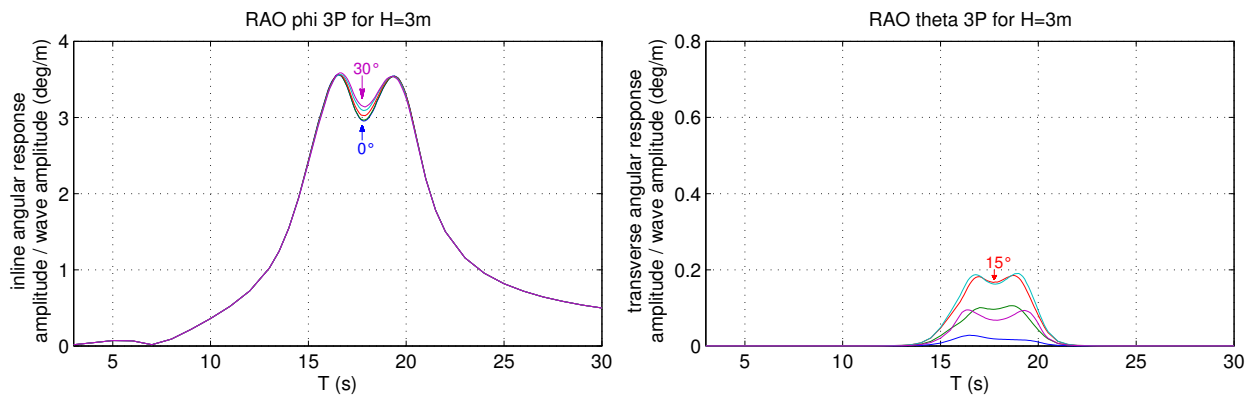
In Fig. 8, we can see that the 3S and 3P systems are more robust against wave incidence than the 2U damper. All dampers create a parasitic transverse



(a) RAO of the 2U system



(b) RAO of the 3S system



(c) RAO of the 3P system

Figure 8: RAO of an arrangement of multiple TLCDs (a) and variants of TLMCDs ((b) and (c)) for different wave incidences of a 3 m monochromatic wave

1
2
3
4
5
6
7
8
9
10
11
12
13
14
15
16
17
18
19
20
21
22
23
24
25
26
27
28
29
30
31
32
33
34
35
36
37
38
39
40
41
42
43
44
45
46
47
48
49
50
51
52
53
54
55
56
57
58
59
60
61
62
63
64
65

1
2
3
4
5 angular response, but it is worth noting that the 2U system creates significantly
6 greater parasitic transverse angular motion than the 3P and 3S dampers.
7

8 **7. Conclusions**

9

10 In this paper, we introduced the concept of a tuned liquid multi-column
11 damper to damp systems with similar pitch and roll behaviours, e.g. an off-
12 shore platform. This damper was inspired by the tuned liquid column damper
13 (TLCD). We developed dynamic models of an offshore platform coupled with
14 different variants of TLMCDs and compared them against a reference system
15 consisting of an arrangement of multiple TLCDs. The results of simulations
16 showed that the two proposed systems (3S and 3P) are more robust against
17 variations in wave incidence than a crosswise layout of two TLCDs.

18 In this study, all considered devices are passive. However further work will
19 focus on the semi-active control of these devices, i.e. changing the head loss
20 coefficients η continually to achieve better performance.
21

22 **References**

- 23
- 24
- 25 [1] C. C. Chang and C. T. Hsu. Control performance of liquid column vi-
26 bration absorbers. *Engineering Structures*, 20(7):580–586, 1998. doi:
27 10.1016/S0141-0296(97)00062-X.
- 28
- 29 [2] S. Christiansen, S. M. Tabatabaeipour, T. Bak, and T. Knudsen. Wave
30 disturbance reduction of a floating wind turbine using a reference model-
31 based predictive control. In *American Control Conference (ACC), 2013*,
32 pages 2214–2219. IEEE, 2013. doi: 10.1109/ACC.2013.6580164.
- 33
- 34 [3] C. Coudurier, O. Lepreux, and N. Petit. Passive and semi-active
35 control of an offshore floating wind turbine using a tuned liquid
36 column damper. *IFAC-PapersOnLine*, 48(16):241–247, 2015. doi:
37 10.1016/j.ifacol.2015.10.287.
- 38
- 39 [4] A. Di Matteo, F. Lo Iacono, G. Navarra, and A. Pirrotta. Direct evaluation
40 of the equivalent linear damping for TLCd systems in random vibration
41 for pre-design purposes. *International Journal of Non-Linear Mechanics*,
42 63:19 – 30, 2014. ISSN 0020-7462. doi: 10.1016/j.ijnonlinmec.2014.03.009.
- 43
- 44 [5] Ernst & Young. Offshore wind in europe: Walking the tightrope to success.
45 Technical report, European Wind Energy Association, 2015.
- 46
- 47 [6] H. Frahm. Results of trials of the anti-rolling tanks at sea. *Journal*
48 *of the American Society for Naval Engineers*, 23(2):571–597, 1911. doi:
49 10.1111/j.1559-3584.1911.tb04595.x.
- 50
- 51 [7] H. Gao, K. Kwok, and B. Samali. Optimization of tuned liquid column
52 dampers. *Engineering Structures*, 19(6):476 – 486, 1997. ISSN 0141-0296.
53 doi: 10.1016/S0141-0296(96)00099-5.
- 54
- 55 [8] C. Holden and T. I. Fossen. A nonlinear 7-dof model for U-
56 tanks of arbitrary shape. *Ocean Engineering*, 45:22–37, 2012. doi:
57 10.1016/j.oceaneng.2012.02.002.
58

- 1
2
3
4
5 [9] International Organization for Standardization. Iso 13624-1-2009 petro-
6 leum and natural gas industries: Drilling and production equipment - part
7 1: Design and operation of marine drilling riser equipment, 2009.
8
9 [10] J. M. Jonkman. *Dynamics modeling and loads analysis of an offshore float-*
10 *ing wind turbine*. PhD thesis, National Renewable Energy Laboratory,
11 2007.
12
13 [11] M. A. Lackner and M. A. Rotea. Structural control of float-
14 ing wind turbines. *Mechatronics*, 21(4):704–719, 2011. doi:
15 10.1016/j.mechatronics.2010.11.007.
16
17 [12] L. Landau and E. Lifshitz. *Mechanics*. Elsevier, third edition, 1976.
18
19 [13] T. J. Larsen and T. D. Hanson. A method to avoid negative damped low
20 frequent tower vibrations for a floating, pitch controlled wind turbine. In
21 *Journal of Physics: Conference Series*, volume 75. IOP Publishing, 2007.
22 doi: 10.1088/1742-6596/75/1/012073.
23
24 [14] N. Luo, C. L. Bottasso, H. R. Karimi, and M. Zapateiro. Semiaactive control
25 for floating offshore wind turbines subject to aero-hydro dynamic loads.
26 *International Conference on Renewable Energies and Power Quality*, 2011.
27
28 [15] R. Moaleji and A. R. Greig. On the development of ship anti-roll
29 tanks. *Ocean Engineering*, 34(1):103 – 121, 2007. ISSN 0029-8018. doi:
30 10.1016/j.oceaneng.2005.12.013.
31
32 [16] W. Musial, S. Butterfield, B. Ram, et al. Energy from offshore wind.
33 In *Offshore technology conference*, pages 1888–1898. Offshore Technology
34 Conference, 2006.
35
36 [17] H. Namik. *Individual blade pitch and disturbance accommodating control*
37 *of floating offshore wind turbines*. PhD thesis, ResearchSpace Auckland,
38 2012.
39
40 [18] H. Namik, M. Rotea, and M. Lackner. Active structural control with ac-
41 tuator dynamics on a floating wind turbine. In *51st AIAA Aerospace Sci-*
42 *ences Meeting including the New Horizons Forum and Aerospace Exposi-*
43 *tion*, 2013. doi: 10.2514/6.2013-455.
44
45 [19] National Renewable Energy Laboratory. *Renewable Energy Data Book*.
46 U.S. Department of Energy, 2012.
47
48 [20] T. Perez and M. Blanke. Ship roll damping control. *Annual Reviews in*
49 *Control*, 36(1):129–147, 2012. doi: 10.1016/j.arcontrol.2012.03.010.
50
51 [21] T. E. Saeed, G. Nikolakopoulos, J.-E. Jonasson, and H. Hedlund. A state-
52 of-the-art review of structural control systems. *Journal of Vibration and*
53 *Control*, 2013. doi: 10.1177/1077546313478294.
54
55 [22] M. Shadman and A. Akbarpour. Utilizing TLCD (tuned liquid column
56 damper) in floating wind turbines. In *ASME 2012 31st International Con-*
57 *ference on Ocean, Offshore and Arctic Engineering*, pages 241–247. Amer-
58 ican Society of Mechanical Engineers, 2012. doi: 10.1115/OMAE2012-
59 83330.
60
61
62
63
64
65

- 1
2
3
4
5 [23] Y. Si, H. R. Karimi, and H. Gao. Modelling and optimization of a
6 passive structural control design for a spar-type floating wind turbine.
7 *Engineering Structures*, 69(0):168 – 182, 2014. ISSN 0141-0296. doi:
8 10.1016/j.engstruct.2014.03.011.
9
10 [24] G. Stewart and M. Lackner. Offshore wind turbine load reduction em-
11 ploying optimal passive tuned mass damping systems. *IEEE trans-*
12 *actions on control systems technology*, 21(4):1090 – 1104, 2013. doi:
13 10.1109/TCST.2013.2260825.
14
15 [25] J.-C. Wu, C.-H. Chang, and Y.-Y. Lin. Optimal designs for non-
16 uniform tuned liquid column dampers in horizontal motion. *Journal of*
17 *Sound and Vibration*, 326(1-2):104 – 122, 2009. ISSN 0022-460X. doi:
18 10.1016/j.jsv.2009.04.027.
19
20 [26] S. Yalla and A. Kareem. Optimum absorber parameters for tuned liquid
21 column dampers. *Journal of Structural Engineering*, 126(8):906–915, 2000.
22 doi: 10.1061/(ASCE)0733-9445(2000)126:8(906).
23
24 [27] S. K. Yalla. *Liquid dampers for mitigation of structural response: theoretical*
25 *development and experimental validation*. PhD thesis, University of Notre
26 Dame, 2001.
27
28
29
30
31
32
33
34
35
36
37
38
39
40
41
42
43
44
45
46
47
48
49
50
51
52
53
54
55
56
57
58
59
60
61
62
63
64
65

Appendix A. Kinetic and potential energy of the proposed dampers

Appendix A.1. Kinetic energy of the NU damper

Following the method used in [8, Appendix B], we compute the kinetic energy of the NU system.

For the NU system and for $i = 1, \dots, N$

$$v_i(\sigma_i) = \frac{A_v}{A_t(\sigma_i)} \dot{w}_i,$$

we write $\mathbf{v}_i^b(\sigma_i)$ according to (1)

$$\mathbf{v}_i^b(\sigma_i) = \frac{A_v}{A_t(\sigma_i)} \dot{w}_i R_z(\alpha_i) \frac{d\mathbf{r}^b}{d\sigma}(\sigma_i).$$

Therefore, matrix $P_{h_{NU}}$ appearing in (2) can be given by

$$P_{h_{NU}} = \nu \mathbb{I}_{nc}$$

We write the kinetic energy of the system as

$$T_{NU} = T_s + T_{DNU},$$

where

$$T_s = \frac{1}{2} v^\top \begin{bmatrix} M_s & 0_{6 \times nc} \\ 0_{nc \times 6} & 0_{nc \times nc} \end{bmatrix} v$$

with M_s the float mass matrix, and

$$\begin{aligned} T_{DNU} &= \frac{1}{2} \rho \sum_{i=1}^N \int_{-\varsigma_{si}}^{\varsigma_{pi}} A_t(\sigma_i) \|\mathbf{v}^b + \omega^b \times R_z(\alpha_i) \mathbf{r}^b(\sigma_i) + \mathbf{v}_i^b(\sigma_i)\|^2 d\sigma_i \\ &= \frac{1}{2} \sum_{i=1}^N \left(\rho \int_{-\varsigma_{si}}^{\varsigma_{pi}} A_t(\sigma_i) d\sigma_i \right) \|\mathbf{v}^b\|^2 - \frac{1}{2} \omega^{b\top} \left(\rho \sum_{i=1}^N \int_{-\varsigma_{si}}^{\varsigma_{pi}} A_t(\sigma_i) S^2(R_z(\alpha_i) \mathbf{r}^b(\sigma_i)) d\sigma_i \right) \omega^b \\ &\quad + \omega^{b\top} \left(\rho \sum_{i=1}^N \int_{-\varsigma_{si}}^{\varsigma_{pi}} A_t(\sigma_i) S(R_z(\alpha_i) \mathbf{r}^b(\sigma_i)) d\sigma_i \right) \mathbf{v}^b + \mathbf{v}^{b\top} \left(\rho A_v \sum_{i=1}^N \int_{-\varsigma_{si}}^{\varsigma_{pi}} R_z(\alpha_i) \frac{d\mathbf{r}^b}{d\sigma}(\sigma_i) \dot{w}_i d\sigma_i \right) \\ &\quad + \omega^{b\top} \left(\rho A_v \sum_{i=1}^N \int_{-\varsigma_{si}}^{\varsigma_{pi}} S(R_z(\alpha_i) \mathbf{r}^b(\sigma_i)) R_z(\alpha_i) \frac{d\mathbf{r}^b}{d\sigma}(\sigma_i) \dot{w}_i d\sigma_i \right) \\ &\quad + \frac{1}{2} \sum_{i=1}^N \left(\rho A_v^2 \int_{-\varsigma_{si}}^{\varsigma_{pi}} \frac{\dot{w}_i^2}{A_t(\sigma_i)} d\sigma_i \right). \end{aligned}$$

Therefore, we can write

$$T_{NU} = \frac{1}{2} v^\top M_{NU}(w) v = \frac{1}{2} \dot{q}^\top \mathcal{M}_{NU}(q) \dot{q}, \quad (\text{A.1})$$

with $\mathcal{M}_{NU} \triangleq \mathcal{P}^\top M_{NU} \mathcal{P}$ and

$$M_{NU}(w) \triangleq \begin{bmatrix} M_s & 0_{6 \times nc} \\ 0_{nc \times 6} & 0_{nc \times nc} \end{bmatrix} + \begin{bmatrix} m_t \mathbb{I}_3 & M_{v\omega}(w) & M_{vq}(w) \\ M_{v\omega}^\top(w) & M_\omega(w) & M_{\omega q}(w) \\ M_{vq}^\top(w) & M_{\omega q}^\top(w) & M_q(w) \end{bmatrix}. \quad (\text{A.2})$$

For $i = 1, \dots, nc$,

$$\begin{aligned}
m_t &\triangleq \rho \sum_{i=1}^N \int_{-\varsigma_{si}}^{\varsigma_{pi}} A_t(\sigma_i) d\sigma_i \in \mathbb{R} \\
M_{v\omega} &\triangleq -\rho \sum_{i=1}^N \int_{-\varsigma_{si}}^{\varsigma_{pi}} A_t(\sigma_i) S(R_z(\alpha_i) \mathbf{r}^b(\sigma_i)) d\sigma_i = -M_{v\omega}^\top(w) \in \mathbb{R}^{3 \times 3} \\
M_\omega &\triangleq -\rho \sum_{i=1}^N \int_{-\varsigma_{si}}^{\varsigma_{pi}} A_t(\sigma_i) S^2(R_z(\alpha_i) \mathbf{r}^b(\sigma_i)) d\sigma_i = M_\omega^\top(w) \in \mathbb{R}^{3 \times 3} \\
M_{vq}[:, i] &\triangleq \rho A_v \int_{-\varsigma_{si}}^{\varsigma_{pi}} R_z(\alpha_i) \frac{d\mathbf{r}^b}{d\sigma}(\sigma_i) d\sigma_i \in \mathbb{R}^{3 \times 1} \\
M_{\omega q}[:, i] &\triangleq \rho A_v \int_{-\varsigma_{si}}^{\varsigma_{pi}} S(R_z(\alpha_i) \mathbf{r}^b(\sigma_i)) R_z(\alpha_i) \frac{d\mathbf{r}^b}{d\sigma}(\sigma_i) d\sigma_i \in \mathbb{R}^{3 \times 1} \\
M_q &\triangleq \mathbb{I}_{nc} \rho A_v (L_h \nu + 2L_v) \in \mathbb{R}^{nc}
\end{aligned}$$

with $M_{vq} \in \mathbb{R}^{3 \times nc}$, $M_{\omega q} \in \mathbb{R}^{3 \times nc}$.

Appendix A.2. Kinetic and potential energy of the NS damper

Following the method used in Appendix A.1 for the NS variant, we write

$$M_{NS}(w) \triangleq \begin{bmatrix} M_s & \mathbf{0}_{6 \times nc} \\ \mathbf{0}_{nc \times 6} & \mathbf{0}_{nc \times nc} \end{bmatrix} + \begin{bmatrix} m_t \mathbb{I}_3 & M_{v\omega}(w) & M_{vq}(w) \\ M_{v\omega}^\top(w) & M_\omega(w) & M_{\omega q}(w) \\ M_{vq}^\top(w) & M_{\omega q}^\top(w) & M_q(w) \end{bmatrix}$$

with, for $j = 1, \dots, nc$,

$$\begin{aligned}
m_t &\triangleq \rho \sum_{i=1}^N \int_0^{\varsigma_i} A_t(\sigma_i) d\sigma_i \in \mathbb{R} \\
M_{v\omega} &\triangleq -\rho \sum_{i=1}^N \int_0^{\varsigma_i} A_t(\sigma_i) S(R_z(\alpha_i) \mathbf{r}^b(\sigma_i)) d\sigma_i = -M_{v\omega}^\top(w) \in \mathbb{R}^{3 \times 3} \\
M_\omega &\triangleq -\rho \sum_{i=1}^N \int_0^{\varsigma_i} A_t(\sigma_i) S^2(R_z(\alpha_i) \mathbf{r}^b(\sigma_i)) d\sigma_i = M_\omega^\top(w) \in \mathbb{R}^{3 \times 3} \\
M_{vq}[:, j] &\triangleq \rho A_v P_{h_{NS}}[:, j] \sum_{i=1}^N \int_0^{\varsigma_i} R_z(\alpha_i) \frac{d\mathbf{r}^b}{d\sigma}(\sigma_i) d\sigma_i \in \mathbb{R}^{3 \times 1} \\
M_{\omega q}[:, j] &\triangleq \rho A_v P_{h_{NS}}[:, j] \sum_{i=1}^N \int_0^{\varsigma_i} S(R_z(\alpha_i) \mathbf{r}^b(\sigma_i)) R_z(\alpha_i) \frac{d\mathbf{r}^b}{d\sigma}(\sigma_i) d\sigma_i \in \mathbb{R}^{3 \times 1} \\
M_q &\triangleq \rho A_v \left(P_{h_{NS}}^\top \frac{L_h}{2\nu} (\nu - 1) + \nu^{-2} P_{h_{NS}}^\top \begin{bmatrix} \varsigma_1 & 0 & \cdots & \cdots & 0 \\ 0 & \ddots & \ddots & & \vdots \\ \vdots & \ddots & \ddots & \ddots & \vdots \\ \vdots & & \ddots & \ddots & 0 \\ 0 & \cdots & \cdots & 0 & \varsigma_N \end{bmatrix} P_{h_{NS}} \right) \in \mathbb{R}^{nc}
\end{aligned}$$

with $M_{vq} \in \mathbb{R}^{3 \times nc}$, $M_{\omega q} \in \mathbb{R}^{3 \times nc}$, and

$$P_{h_{NS}} \triangleq \nu \begin{bmatrix} \mathbb{I}_{nc} \\ -\mathbb{1}_{1 \times nc} \end{bmatrix}.$$

The potential energy of the NS system is written as

$$\begin{aligned} V_{NS} &= \mathbf{z}^\top \cdot \left(g\rho \sum_{i=1}^N \int_0^{\varsigma_i} A_t(\sigma) (R(\Theta) R_z(\alpha_i) \mathbf{r}^b(\sigma) + \mathbf{x}^n) d\sigma \right) \\ &= -gm_t z - g\rho \mathbf{z}^\top R(\Theta) \left[\rho \sum_{i=1}^N \int_0^{\varsigma_i} A_t(\sigma) R_z(\alpha_i) \mathbf{r}^b(\sigma) d\sigma \right] \end{aligned} \quad (\text{A.3})$$

Appendix A.3. Kinetic and potential energy of the NP damper

Following the method used in Appendix A.1 for the NP variant, we write

$$M_{NP}(w) \triangleq \begin{bmatrix} M_s & \mathbf{0}_{6 \times nc} \\ \mathbf{0}_{nc \times 6} & \mathbf{0}_{nc \times nc} \end{bmatrix} + \begin{bmatrix} m_t \mathbb{I}_3 & M_{v\omega}(w) & M_{vq}(w) \\ M_{v\omega}^\top(w) & M_\omega(w) & M_{\omega q}(w) \\ M_{vq}^\top(w) & M_{\omega q}^\top(w) & M_q(w) \end{bmatrix}$$

with, for $j = 1, \dots, nc$,

$$\begin{aligned} m_t &\triangleq \rho \sum_{i=1}^N \int_{-\frac{L_h}{2}}^{\varsigma_i} A_t(\sigma_i) d\sigma_i \in \mathbb{R} \\ M_{v\omega} &\triangleq -\rho \sum_{i=1}^N \int_{-\frac{L_h}{2}}^{\varsigma_i} A_t(\sigma_i) S(R_z(\alpha_i) \mathbf{r}^b(\sigma_i)) d\sigma_i = -M_{v\omega}^\top(w) \in \mathbb{R}^{3 \times 3} \\ M_\omega &\triangleq -\rho \sum_{i=1}^N \int_{-\frac{L_h}{2}}^{\varsigma_i} A_t(\sigma_i) S^2(R_z(\alpha_i) \mathbf{r}^b(\sigma_i)) d\sigma_i = M_\omega^\top(w) \in \mathbb{R}^{3 \times 3} \\ M_{vq}[:, j] &\triangleq \rho A_v P_{h_{NP}}[:, j] \sum_{i=1}^N \int_{-\frac{L_h}{2}}^{\frac{L_h}{2}} R_z(\alpha_i) \frac{d\mathbf{r}^b}{d\sigma}(\sigma_i) d\sigma_i \\ &\quad + \rho A_v P_{h_{2NP}}[:, j] \sum_{i=1}^N \int_{\frac{L_h}{2}}^{\varsigma_i} R_z(\alpha_i) \frac{d\mathbf{r}^b}{d\sigma}(\sigma_i) d\sigma_i \in \mathbb{R}^{3 \times 1} \\ M_{\omega q}[:, j] &\triangleq \rho A_v P_{h_{NP}}[:, j] \sum_{i=1}^N \int_{-\frac{L_h}{2}}^{\frac{L_h}{2}} S(R_z(\alpha_i) \mathbf{r}^b(\sigma_i)) R_z(\alpha_i) \frac{d\mathbf{r}^b}{d\sigma}(\sigma_i) d\sigma_i \\ &\quad + \rho A_v P_{h_{2NP}}[:, j] \sum_{i=1}^N \int_{\frac{L_h}{2}}^{\varsigma_i} S(R_z(\alpha_i) \mathbf{r}^b(\sigma_i)) R_z(\alpha_i) \frac{d\mathbf{r}^b}{d\sigma}(\sigma_i) d\sigma_i \in \mathbb{R}^{3 \times 1} \\ M_q &\triangleq \rho A_v \left(\frac{L_h}{\nu} P_{h_{NP}}^\top P_{h_{NP}} + \nu^{-2} P_{h_{2NP}}^\top \begin{bmatrix} \varsigma_1 - \frac{L_h}{2} & 0 & \cdots & \cdots & 0 \\ 0 & \ddots & \ddots & & \vdots \\ \vdots & \ddots & \ddots & \ddots & \vdots \\ \vdots & & \ddots & \ddots & 0 \\ 0 & \cdots & \cdots & 0 & \varsigma_N - \frac{L_h}{2} \end{bmatrix} P_{h_{2NP}} \right) \in \mathbb{R}^{nc} \end{aligned}$$

with $M_{vq} \in \mathbb{R}^{3 \times nc}$, $M_{\omega q} \in \mathbb{R}^{3 \times nc}$, and

$$P_{h2NP} \triangleq \begin{bmatrix} \mathbb{I}_{N-1} & 0_{N-1 \times 1} \\ -\mathbb{1}_{1 \times N-1} & 0 \end{bmatrix}$$

$$P_{hNP} \triangleq \begin{bmatrix} \nu & 0 & \cdots & 0 & 1 \\ \nu & \ddots & \ddots & \vdots & \vdots \\ \vdots & \ddots & \ddots & 0 & 1 \\ \nu & \cdots & \nu & \nu & 1 \\ 0 & \cdots & 0 & 0 & 1 \end{bmatrix}.$$

The potential energy of the NP system is written as

$$V_{NP} = \mathbf{z}^\top \cdot \left(g\rho \sum_{i=1}^N \int_{-\frac{L_h}{2}}^{\varsigma_i} A_t(\sigma) (R(\Theta) R_z(\alpha_i) \mathbf{r}^b(\sigma) + \mathbf{x}^n) d\sigma \right)$$

$$= -gm_t z - g\rho \mathbf{z}^\top R(\Theta) \left[\rho \sum_{i=1}^N \int_{-\frac{L_h}{2}}^{\varsigma_i} A_t(\sigma) R_z(\alpha_i) \mathbf{r}^b(\sigma) d\sigma \right] \quad (\text{A.4})$$

Appendix B. Derivation of system dynamics

Appendix B.1. Preliminary results

For our calculation, we need the following results:

We define the derivative of row vector $x^\top \triangleq [x_1 \ \dots \ x_n]$ by column

vector $y \triangleq \begin{bmatrix} y_1 \\ \vdots \\ y_m \end{bmatrix}$ as

$$\frac{\partial x^\top}{\partial y} \triangleq \begin{bmatrix} \frac{\partial x_1}{\partial y_1} & \cdots & \frac{\partial x_n}{\partial y_1} \\ \vdots & \ddots & \vdots \\ \frac{\partial x_1}{\partial y_m} & \cdots & \frac{\partial x_n}{\partial y_m} \end{bmatrix}. \quad (\text{B.1})$$

Proposition 1. $\forall \mathbf{r} \in \mathbb{R}^3$, the derivative of $\mathbf{r}^\top R$ by Θ is given as

$$\frac{\partial \mathbf{r}^\top R}{\partial \Theta} = -G^\top S(R^\top \mathbf{r}) \quad (\text{B.2})$$

with G as defined in (??), and $S(\cdot)$ is the matrix associated with the cross-product.

Proof. We detail the calculus for each of the tree base vectors $(\mathbf{x}, \mathbf{y}, \mathbf{z})$. We have

$$R^\top \mathbf{z} = \begin{bmatrix} -s_\theta \\ s_\varphi c_\theta \\ c_\varphi c_\theta \end{bmatrix}$$

so

$$-G^\top S(R^\top \mathbf{z}) = \begin{bmatrix} 0 & c_\theta c_\varphi & -c_\theta s_\varphi \\ -c_\theta & -s_\theta s_\varphi & -s_\theta c_\varphi \\ 0 & 0 & 0 \end{bmatrix}$$

and

$$\frac{\partial \mathbf{z}^\top R}{\partial \Theta} = \begin{bmatrix} 0 & c_\theta c_\varphi & -c_\theta s_\varphi \\ -c_\theta & -s_\theta s_\varphi & -s_\theta c_\varphi \\ 0 & 0 & 0 \end{bmatrix}.$$

Therefore,

$$\frac{\partial \mathbf{z}^\top R}{\partial \Theta} = -G^\top S (R^\top \mathbf{z}).$$

We also have

$$R^\top \mathbf{y} = \begin{bmatrix} c_\theta s_\psi \\ c_\varphi c_\psi + s_\varphi s_\theta s_\psi \\ -s_\varphi c_\psi + c_\varphi s_\theta s_\psi \end{bmatrix}$$

so,

$$-G^\top S (R^\top \mathbf{y}) = \begin{bmatrix} 0 & -s_\varphi c_\psi + c_\varphi s_\theta s_\psi & -c_\varphi c_\psi - s_\varphi s_\theta s_\psi \\ -s_\theta s_\psi & s_\varphi c_\theta s_\psi & c_\varphi c_\theta s_\psi \\ c_\theta c_\psi & -c_\varphi s_\psi + s_\varphi s_\theta c_\psi & s_\varphi s_\psi + c_\varphi s_\theta c_\psi \end{bmatrix}$$

and

$$\frac{\partial \mathbf{y}^\top R}{\partial \Theta} = \begin{bmatrix} 0 & -s_\varphi c_\psi + c_\varphi s_\theta s_\psi & -c_\varphi c_\psi - s_\varphi s_\theta s_\psi \\ -s_\theta s_\psi & s_\varphi c_\theta s_\psi & c_\varphi c_\theta s_\psi \\ c_\theta c_\psi & -c_\varphi s_\psi + s_\varphi s_\theta c_\psi & s_\varphi s_\psi + c_\varphi s_\theta c_\psi \end{bmatrix}.$$

Therefore,

$$\frac{\partial \mathbf{y}^\top R}{\partial \Theta} = -G^\top S (R^\top \mathbf{y}).$$

Finally,

$$R^\top \mathbf{x} = \begin{bmatrix} c_\theta c_\psi \\ -c_\varphi s_\psi + s_\varphi s_\theta c_\psi \\ s_\varphi s_\psi + c_\varphi s_\theta c_\psi \end{bmatrix}$$

so,

$$-G^\top S (R^\top \mathbf{x}) = \begin{bmatrix} 0 & s_\varphi s_\psi + c_\varphi s_\theta c_\psi & c_\varphi s_\psi - s_\varphi s_\theta c_\psi \\ -s_\theta c_\psi & s_\varphi c_\theta c_\psi & c_\varphi c_\theta c_\psi \\ -c_\theta s_\psi & -c_\varphi c_\psi - s_\varphi s_\theta s_\psi & s_\varphi c_\psi - c_\varphi s_\theta s_\psi \end{bmatrix}$$

and

$$\frac{\partial \mathbf{x}^\top R}{\partial \Theta} = \begin{bmatrix} 0 & s_\varphi s_\psi + c_\varphi s_\theta c_\psi & c_\varphi s_\psi - s_\varphi s_\theta c_\psi \\ -s_\theta c_\psi & s_\varphi c_\theta c_\psi & c_\varphi c_\theta c_\psi \\ -c_\theta s_\psi & -c_\varphi c_\psi - s_\varphi s_\theta s_\psi & s_\varphi c_\psi - c_\varphi s_\theta s_\psi \end{bmatrix}.$$

Therefore,

$$\frac{\partial \mathbf{x}^\top R}{\partial \Theta} = -G^\top S (R^\top \mathbf{x}).$$

With $\mathbf{r} = r_1 \mathbf{x} + r_2 \mathbf{y} + r_3 \mathbf{z}$, by linearity,

$$\frac{\partial \mathbf{r}^\top R}{\partial \Theta} = -G^\top S (R^\top \mathbf{r}).$$

□

Proposition 2. *The derivatives of $\mathbf{v}^{b\top}$ and $\omega^{b\top}$ by Θ are*

$$\frac{\partial \mathbf{v}^{b\top}}{\partial \Theta} = -G^\top S(\mathbf{v}^b) \quad (\text{B.3})$$

$$\frac{\partial \omega^{b\top}}{\partial \Theta} = \dot{G}^\top - G^\top S(\omega^b). \quad (\text{B.4})$$

Proof. Hence,

$$\omega^b = G(\Theta) \dot{\Theta} = \begin{bmatrix} \dot{\varphi} + s_\theta \dot{\psi} \\ c_\theta s_\varphi \dot{\psi} + c_\varphi \dot{\theta} \\ c_\theta c_\varphi \dot{\psi} - s_\varphi \dot{\theta} \end{bmatrix}$$

so,

$$\frac{\partial \omega^{b\top}}{\partial \Theta} = \begin{bmatrix} 0 & c_\theta c_\varphi \dot{\psi} - s_\varphi \dot{\theta} & -c_\theta s_\varphi \dot{\psi} - c_\varphi \dot{\theta} \\ -c_\theta \dot{\psi} & -s_\theta s_\varphi \dot{\psi} & -s_\theta c_\varphi \dot{\psi} \\ 0 & 0 & 0 \end{bmatrix}$$

With G as defined in (??),

$$\dot{G}^\top = \begin{bmatrix} 0 & 0 & 0 \\ 0 & -s_\varphi \dot{\varphi} & -c_\varphi \dot{\theta} \\ -c_\theta \dot{\theta} & c_\theta c_\varphi \dot{\varphi} - s_\theta s_\varphi \dot{\theta} & -c_\theta s_\varphi \dot{\varphi} - s_\theta c_\varphi \dot{\theta} \end{bmatrix}.$$

We also write

$$G^\top S(G(\Theta) \dot{\Theta}) = \begin{bmatrix} 0 & -c_\theta c_\varphi \dot{\psi} + s_\varphi \dot{\theta} & c_\theta s_\varphi \dot{\psi} + c_\varphi \dot{\theta} \\ c_\theta \dot{\psi} & s_\varphi (-\dot{\varphi} + s_\theta \dot{\psi}) & c_\varphi (-\dot{\varphi} + s_\theta \dot{\psi}) \\ -c_\theta \dot{\theta} & c_\theta c_\varphi \dot{\varphi} - s_\theta s_\varphi \dot{\theta} & -c_\theta s_\varphi \dot{\varphi} - s_\theta c_\varphi \dot{\theta} \end{bmatrix}.$$

Therefore,

$$\frac{\partial \omega^{b\top}}{\partial \Theta} = \dot{G}^\top - G^\top S(\omega^b).$$

As \mathbf{v}^b is $R^\top \dot{\mathbf{x}}^e$, according to Proposition 1,

$$\frac{\partial \mathbf{v}^{b\top}}{\partial \Theta} = -G^\top S(\mathbf{v}^b).$$

□

Appendix B.2. Derivation of the dynamics for the NU system

Using a Lagrangian approach, the dynamics of the system are given by

$$\frac{d}{dt} \frac{\partial (T_{NU} - V_{NU})}{\partial \dot{q}} - \frac{\partial (T_{NU} - V_{NU})}{\partial q} = Q$$

We first derive $\frac{\partial T_{NU}}{\partial q}$. According to (A.1), T is independent of x^n ; therefore,

$$\frac{\partial T_{NU}}{\partial x^n} = 0_{3 \times 1}.$$

As M is symmetrical and is not a function of Θ ,

$$\frac{\partial T_{NU}}{\partial \Theta} = \frac{1}{2} \frac{\partial (\dot{q}^\top \mathcal{P}^\top M_{NU} \mathcal{P} \dot{q})}{\partial \Theta} = \frac{\partial (\mathcal{P} \dot{q})^\top}{\partial \Theta} M_{NU} (\mathcal{P} \dot{q}).$$

Using (B.3) and (B.4),

$$\frac{\partial (\mathcal{P} \dot{q})^\top}{\partial \Theta} = \frac{\partial v^\top}{\partial \Theta} = \left[\frac{\partial \mathbf{v}^{b\top}}{\partial \Theta}, \frac{\partial \omega^{b\top}}{\partial \Theta}, 0_{3 \times 1} \right] = \left[-G^\top S(\mathbf{v}^b) \quad \dot{G}^\top - G^\top S(\omega^b) \quad 0_{3 \times 1} \right].$$

The term $\frac{\partial T}{\partial w_i}$ can be expressed as

$$\frac{\partial T_{NU}}{\partial w_i} = \frac{1}{2} \dot{q}^\top \mathcal{P}^\top \frac{\partial M_{NU}}{\partial w_i} \mathcal{P} \dot{q}$$

with

$$\begin{aligned} \frac{\partial}{\partial w_i} M_{v\omega} &= -\rho A_v S \left(R_z(\alpha_i) \mathbf{r}^b(\varsigma_{pi}) - R_z(\alpha_i) \mathbf{r}^b(-\varsigma_{si}) \right) \\ \frac{\partial}{\partial w_i} M_\omega &= -\rho A_v \left(S \left(R_z(\alpha_i) \mathbf{r}^b(\varsigma_{pi}) \right)^2 - S \left(R_z(\alpha_i) \mathbf{r}^b(-\varsigma_{si}) \right)^2 \right) \\ \frac{\partial}{\partial w_i} M_{vq}[:, i] &= \rho A_v \left(R_z(\alpha_i) \frac{d\mathbf{r}^b}{d\sigma}(\varsigma_{pi}) - R_z(\alpha_i) \frac{d\mathbf{r}^b}{d\sigma}(-\varsigma_{si}) \right) \\ \frac{\partial}{\partial w_i} M_{vq}[:, j \neq i] &= 0_{3 \times 1} \\ \frac{\partial}{\partial w_i} M_{\omega q}[:, i] &= \rho A_v \left(S \left(R_z(\alpha_i) \mathbf{r}^b(\varsigma_{pi}) \right) R_z(\alpha_i) \frac{d\mathbf{r}^b}{d\sigma}(\varsigma_{pi}) - S \left(R_z(\alpha_i) \mathbf{r}^b(-\varsigma_{si}) \right) R_z(\alpha_i) \frac{d\mathbf{r}^b}{d\sigma}(-\varsigma_{si}) \right) \\ \frac{\partial}{\partial w_i} M_{\omega q}[:, j \neq i] &= 0_{3 \times 1} \\ \frac{\partial}{\partial w_i} M_q &= 0_{nc \times nc}. \end{aligned}$$

According to (5), and (B.2), $\frac{\partial V_{NU}}{\partial q}$ is given by

$$\begin{aligned} \frac{\partial V_{NU}}{\partial x^n} &= \begin{bmatrix} 0 \\ 0 \\ -gm_t \end{bmatrix} = -gm_t \mathbf{z} \\ \frac{\partial V_{NU}}{\partial \Theta} &= -g\rho \frac{\partial \mathbf{z}^\top R}{\partial \Theta} \left(\sum_{i=1}^{nc} \int_{-\varsigma_{si}}^{\varsigma_{pi}} A_t(\sigma) R_z(\alpha_i) \mathbf{r}^b(\sigma) d\sigma \right) \\ &= g\rho G^\top S \left(R^\top \mathbf{z} \right) \left(\sum_{i=1}^{nc} \int_{-\varsigma_{si}}^{\varsigma_{pi}} A_t(\sigma) R_z(\alpha_i) \mathbf{r}^b(\sigma) d\sigma \right) \\ &= g\rho G^\top S \left(R^\top \mathbf{z} \right) \left(A_h \sum_{i=1}^{nc} \begin{bmatrix} \nu L_h w_i \sin \alpha_i \\ -\nu L_h w_i \cos \alpha_i \\ \nu (2L_v e - L_v^2 - w_i^2) + L_h e \end{bmatrix} \right) \\ \frac{\partial V_{NU}}{\partial w_i} &= -g\rho A_v \mathbf{z}^\top R(\Theta) R_z(\alpha_i) \left(\mathbf{r}^b(\varsigma_{pi}) - \mathbf{r}^b(-\varsigma_{si}) \right). \end{aligned}$$

According to (5), V_{NU} is not a function of \dot{q} ; thus,

$$\frac{d}{dt} \frac{\partial V_{NU}}{\partial \dot{q}} = 0_{6+nc \times 1}.$$

We also have

$$\frac{d}{dt} \left(\frac{\partial T_{NU}}{\partial \dot{q}} \right)^\top = \mathcal{M}_{NU} \ddot{q} + \left(\dot{\mathcal{P}}^\top M_{NU} \mathcal{P} + \mathcal{P}^\top \sum_{i=1}^{nc} \dot{w}_i \frac{\partial M_{NU}}{\partial w_i} \mathcal{P} + \mathcal{P}^\top M_{NU} \dot{\mathcal{P}} \right) \dot{q}.$$

Appendix B.3. Summary of NU system dynamics

We write the dynamics of the system as

$$\mathcal{M}_{NU}(q) \ddot{q} + C_{NU}(q, \dot{q}) \dot{q} + k_{NU}(q) = Q_{hydro}(t, \beta) + Q_{res_{NU}}(\dot{w})$$

with $\mathcal{M}_{NU}(q)$ defined in (A.1), and

$$C_{NU} \triangleq \dot{\mathcal{P}}^\top M_{NU} \mathcal{P} + \mathcal{P}^\top \sum_{i=1}^{nc} \dot{w}_i \frac{\partial M_{NU}}{\partial w_i} \mathcal{P} + \mathcal{P}^\top M_{NU} \dot{\mathcal{P}} - \begin{bmatrix} 0_{3 \times 6 + nc} \\ \frac{\partial(\mathcal{P} \dot{q})^\top}{\partial \Theta} M_{NU} \mathcal{P} \\ \frac{1}{2} \dot{q}^\top \mathcal{P}^\top \frac{\partial M_{NU}}{\partial w_1} \mathcal{P} \\ \vdots \\ \frac{1}{2} \dot{q}^\top \mathcal{P}^\top \frac{\partial M_{NU}}{\partial w_{nc}} \mathcal{P} \end{bmatrix}$$

$$k_{NU} \triangleq -g \begin{bmatrix} m_t \mathbf{z} \\ -\rho G^\top S (R^\top \mathbf{z}) \sum_{i=1}^{nc} \int_{-\zeta_{s_i}}^{\zeta_{p_i}} A_t(\sigma) R_z(\alpha_i) \mathbf{r}^b(\sigma) d\sigma \\ \rho A_v \mathbf{z}^\top R(\Theta) R_z(\alpha_1) (\mathbf{r}^b(\zeta_{p1}) - \mathbf{r}^b(-\zeta_{s1})) \\ \vdots \\ \rho A_v \mathbf{z}^\top R(\Theta) R_z(\alpha_{nc}) (\mathbf{r}^b(\zeta_{pnc}) - \mathbf{r}^b(-\zeta_{snc})) \end{bmatrix}$$

$$Q_{res_{NU}} = \begin{bmatrix} 0_{1 \times 6} \\ P_{h_{NU}}^\top F_h(\dot{w}) \end{bmatrix}$$

$$P_{h_{NU}} = \nu \mathbb{I}_{nc}.$$

Appendix B.4. Summary of NS system dynamics

Using the expressions of the energies obtained in Appendix A.2, and following the method used in Appendix B for the NU system, we write the dynamics of the NS system as

$$\mathcal{M}_{NS}(q) \ddot{q} + C_{NS}(q, \dot{q}) \dot{q} + k_{NS}(q) = Q_{hydro}(t, \beta) + Q_{res_{NS}}(\dot{w})$$

with

$$\mathcal{M}_{NS}(q) \triangleq \mathcal{P}(\Theta)^\top M_{NS}(w) \mathcal{P}(\Theta)$$

$$C_{NS} \triangleq \dot{\mathcal{P}}^\top M_{NS} \mathcal{P} + \mathcal{P}^\top \sum_{i=1}^{nc} \dot{w}_i \frac{\partial M_{NS}}{\partial w_i} \mathcal{P} + \mathcal{P}^\top M_{NS} \dot{\mathcal{P}} - \begin{bmatrix} 0_{3 \times 6 + nc} \\ \frac{\partial(\mathcal{P} \dot{q})^\top}{\partial \Theta} M_{NS} \mathcal{P} \\ \frac{1}{2} \dot{q}^\top \mathcal{P}^\top \frac{\partial M_{NS}}{\partial w_1} \mathcal{P} \\ \vdots \\ \frac{1}{2} \dot{q}^\top \mathcal{P}^\top \frac{\partial M_{NS}}{\partial w_{nc}} \mathcal{P} \end{bmatrix}$$

$$k_{NS} \triangleq -g \begin{bmatrix} m_t \mathbf{z} \\ -\rho G^\top S (R^\top \mathbf{z}) \sum_{i=1}^N \int_0^{\zeta_i} A_t(\sigma) R_z(\alpha_i) \mathbf{r}^b(\sigma) d\sigma \\ \rho A_v \mathbf{z}^\top R(\Theta) (R_z(\alpha_1) \mathbf{r}^b(\zeta_1) - R_z(\alpha_N) \mathbf{r}^b(\zeta_N)) \\ \vdots \\ \rho A_v \mathbf{z}^\top R(\Theta) (R_z(\alpha_{nc}) \mathbf{r}^b(\zeta_{nc}) - R_z(\alpha_N) \mathbf{r}^b(\zeta_N)) \end{bmatrix}$$

$$Q_{res_{NS}} = \begin{bmatrix} 0_{1 \times 6} \\ P_{h_{NS}}^\top F_h(\dot{w}) \end{bmatrix}$$

$$P_{h_{NS}} = \nu \begin{bmatrix} \mathbb{I}_{nc} \\ -\mathbb{1}_{1 \times nc} \end{bmatrix}.$$

Appendix B.5. Summary of NP system dynamics

Using the expressions of the energies obtained in Appendix A.3, and following the method used in Appendix B for the NU system, we write the dynamics of the NP system as

$$\mathcal{M}_{NP}(q) \ddot{q} + C_{NP}(q, \dot{q}) \dot{q} + k_{NP}(q) = Q_{hydro} + Q_{res_{NP}}(\dot{w})$$

with

$$\mathcal{M}_{NP}(q) \triangleq \mathcal{P}(\Theta)^\top M_{NP}(w) \mathcal{P}(\Theta)$$

$$C_{NP} \triangleq \dot{\mathcal{P}}^\top M_{NP} \mathcal{P} + \mathcal{P}^\top \sum_{i=1}^{nc} \dot{w}_i \frac{\partial M_{NP}}{\partial w_i} \mathcal{P} + \mathcal{P}^\top M_{NP} \dot{\mathcal{P}} - \begin{bmatrix} 0_{3 \times 6 + nc} \\ \frac{\partial(\mathcal{P} \dot{q})^\top}{\partial \Theta} M_{NP} \mathcal{P} \\ \frac{1}{2} \dot{q}^\top \mathcal{P}^\top \frac{\partial M_{NP}}{\partial w_1} \mathcal{P} \\ \vdots \\ \frac{1}{2} \dot{q}^\top \mathcal{P}^\top \frac{\partial M_{NP}}{\partial w_{nc-1}} \mathcal{P} \\ 0_{1 \times 6 + nc} \end{bmatrix}$$

$$k_{NP} \triangleq -g \begin{bmatrix} m_t \mathbf{z} \\ -\rho G^\top S(R^\top \mathbf{z}) \sum_{i=1}^N \int_{-\frac{L_h}{2}}^{\zeta_i} A_t(\sigma) R_z(\alpha_i) \mathbf{r}^b(\sigma) d\sigma \\ \rho A_v \mathbf{z}^\top R(\Theta) (R_z(\alpha_1) \mathbf{r}^b(\zeta_1) - R_z(\alpha_N) \mathbf{r}^b(\zeta_N)) \\ \vdots \\ \rho A_v \mathbf{z}^\top R(\Theta) (R_z(\alpha_{N-1}) \mathbf{r}^b(\zeta_{N-1}) - R_z(\alpha_N) \mathbf{r}^b(\zeta_N)) \\ 0 \end{bmatrix}$$

$$Q_{res_{NP}} = \begin{bmatrix} 0_{1 \times 6} \\ P_{h_{NP}}^\top F_h(\dot{w}) \end{bmatrix}$$

$$P_{h_{NP}} = \begin{bmatrix} \nu & 0 & \cdots & 0 & 1 \\ \nu & \ddots & \ddots & \vdots & \vdots \\ \vdots & \ddots & \ddots & 0 & 1 \\ \nu & \cdots & \nu & \nu & 1 \\ 0 & \cdots & 0 & 0 & 1 \end{bmatrix}.$$